MITSUBISHI ELECTRIC RESEARCH LABORATORIES https://www.merl.com

Set-based lossless convexification for a class of robust nonlinear optimal control problems

Vinod, Abraham P.; Kamath, Abhinav; Weiss, Avishai; Di Cairano, Stefano TR2025-160 November 07, 2025

Abstract

We introduce a set-based, globally optimal con- troller for a specific class of nonlinear robust optimal control problems (ROCP). Traditional dynamic programming methods for solving nonlinear ROCP to global optimality require space discretization, leading to the well-known curse of dimensional- ity. In this paper, we establish sufficient conditions under which a convex relaxation of the dynamic programming recursion for a nonlinear ROCP is lossless, meaning it recovers the globally optimal solution of the original, non-convex recursion. We propose a computationally tractable, space discretization- free, almost lossless implementation of our approach using constrained zonotopes and a series of convex one-step optimal control problems. Additionally, we provide a suboptimality bound for the controller derived from our method for a standard nonlinear ROCP.

IEEE Conference on Decision and Control (CDC) 2025

^{© 2025} IEEE. Personal use of this material is permitted. Permission from IEEE must be obtained for all other uses, in any current or future media, including reprinting/republishing this material for advertising or promotional purposes, creating new collective works, for resale or redistribution to servers or lists, or reuse of any copyrighted component of this work in other works.

Set-based lossless convexification for a class of robust nonlinear optimal control problems

Abraham P. Vinod*, Abhinav G. Kamath, Avishai Weiss, and Stefano Di Cairano

Abstract—We introduce a set-based, globally optimal controller for a specific class of nonlinear robust optimal control problems (ROCP). Traditional dynamic programming methods for solving nonlinear ROCP to global optimality require space discretization, leading to the well-known curse of dimensionality. In this paper, we establish sufficient conditions under which a convex relaxation of the dynamic programming recursion for a nonlinear ROCP is lossless, meaning it recovers the globally optimal solution of the original, non-convex recursion. We propose a computationally tractable, space discretization-free, almost lossless implementation of our approach using constrained zonotopes and a series of convex one-step optimal control problems. Additionally, we provide a suboptimality bound for the controller derived from our method for a standard nonlinear ROCP.

I. INTRODUCTION

Nonlinear robust optimal control problems (ROCP) arise while designing optimal controllers for physical systems subject to uncertainties and constraints [1]–[4]. Existing literature tackles these control problems using a variety of approaches, including dynamic programming [1] and nonlinear robust model predictive control (MPC) [2]. Unfortunately, these approaches may suffer from computational difficulties arising from space discretization or may yield conservative (i.e., suboptimal) controllers in order to tractably guarantee robust constraint satisfaction. This paper proposes theory and tractable algorithms to solve a class of nonlinear ROCP to global optimality using recent results from computational geometry and dynamic programming.

Nonlinear ROCP may be analyzed using the framework of dynamic programming [1]. Specifically, using the Bellman optimality principle, we can (recursively) define a set of value functions for the ROCP and design deterministic, state-feedback controllers that are provably optimal. However, implementations of such dynamic programming-based approaches often require space discretization which limits the approach to smaller dimensional systems [1], or require approximate dynamic programming techniques that come with a loss of robust constraint satisfaction guarantees [5]. For certain specific nonlinear systems (e.g. piecewise-affine systems), a set-theoretic approach based on dynamic programming and parametric programming has been considered, but may require significant computational effort [6].

Locally optimal or suboptimal solutions to nonlinear ROCP may be obtained using robust model predictive control (MPC) [2], [3], including tube MPC and minmax MPC. Tube MPC approaches typically reformulate the ROCP into a single optimization problem over the control actions, and enforce tightened constraints on the resulting nominal trajectory to account for the effect of disturbance [7], [8]. Compared to tube MPC, minmax MPC explicitly considers the disturbances in the controller design when optimizing for control actions, but typically require higher computational effort [2], [9]-[11]. Popular minmax MPC techniques include two-player games [10], the enumeration of disturbance scenarios for polytopic disturbance sets [12], and solving multiparametric programs [13]. In general, most of the existing MPC-based approaches focus on generating tractable but suboptimal solutions due to the inherent non-convexity in the ROCP. In this work, we propose a tractable method to solve a class of nonlinear ROCP to (almost) global optimality using computational geometry and dynamic programming.

The main contribution of this paper is a set-based control design framework to compute globally optimal controllers for a class of nonlinear ROCP. Specifically, we identify a class of nonlinear ROCP for which the convex relaxation of their dynamic programming recursion is lossless, i.e., the convex relaxation recovers the globally optimal solution for the original, non-convex dynamic programming recursion. Additionally, we show that the control design may be accomplished via a series of convex, one-step optimal control problems and a collection of set operations tractably and almost losslessly implemented using constrained zonotopes. Finally, we provide a suboptimality bound on the controller computed using the proposed approach for a standard formulation of a nonlinear ROCP. We also prove that the robust controllable sets for the considered class of nonlinear ROCP are convex, and demonstrate our approach on a 7D ROCP.

We remark that our problem of interest and solution approach are quite different from existing *lossless convexification* methods in trajectory generation problems [14]–[16], where globally optimal solutions to continuous-time, nonlinear, disturbance-free optimal control problems are obtained from convex relaxations using the *Pontryagin maximum principle*. Instead, our approach solves discrete-time, nonlinear ROCP using dynamic programming and set-based control.

Furthermore, a related problem to the nonlinear ROCP considered in this paper is the computation of so-called *robust controllable sets*. A robust controllable set is a set of initial states from which the system may be steered to satisfy state-input constraints despite the uncertainty acting

^{*}Corresponding author. Email: {abraham.p.vinod}@ieee.org. A. P. Vinod, A. Weiss, and S. Di Cairano are with Mitsubishi Electric Research Laboratories (MERL), Cambridge, MA 02139, USA.

A. G. Kamath is a Ph.D. Student, William E. Boeing Department of Aeronautics & Astronautics, University of Washington, Seattle, WA 98195, USA. This work was completed during Mr. Kamath's internship at MERL.

on the system [4], [17]. For linear dynamics with additive uncertainty and polytopic constraints, these sets may be computed by a set recursion on polytopes, using existing tools for computational geometry [18]–[20]. Recent progress in constrained zonotopes [21], [22], an equivalent representation for polytopes, has enabled tractable computation of robust controllable sets for high-dimensional linear systems subject to polytopic constraints and additive, symmetric, convex, and compact disturbance sets (e.g., ellipsoids and zonotopes). A key insight used in our approach is that the convex relaxation of the dynamic programming for certain ROCP may be analyzed using robust controllable sets, which mitigates the curse of dimensionality in space discretizationbased dynamic programming. In this paper, we perform all set-based computations using constrained zonotopes for computational efficiency.

Notation: $0_{n\times m}$ and $1_{n\times m}$ are matrices of zeros and ones in $\mathbb{R}^{n\times m}$ respectively, I_n is the n-dimensional identity matrix, $\mathbb{N}_{[a,b]}$ is the subset of natural numbers between (and including) $a,b\in\mathbb{N},\ a\leq b,$ and $\|\cdot\|_p$ is the p-norm of a vector. Let M be a matrix and M_1 (M_2 , resp.) be another matrix of the same height (width, resp.) as M. Then, $[M,M_1]$ ($[M;M_2]$, resp.) denotes the matrix obtained by concatenating M and M_1 horizontally (concatenating M and M_2 vertically, resp.). We concatenate vectors v_1,v_2 by $[v_1;v_2]$, and denote component-wise inequalities by $v_1\leq v_2$ or $v_1\geq v_2$. Finally, v_i is the i^{th} component of a vector $v\in\mathbb{R}^n$, and M_i is the i^{th} column of a matrix M.

II. PRELIMINARIES

We now briefly review relevant mathematical background and set up the problem statements of interest.

A. Real analysis and optimization

For a set $S \subseteq \mathbb{R}^n$, we denote its indicator function by $\mathbb{I}_S : \mathbb{R}^n \to \{0,\infty\}$, with $\mathbb{I}_S(x) = 0$ when $x \in S$, and ∞ otherwise. For a function $f : \mathbb{R}^n \to \mathbb{R}$, we denote its epigraph by $\mathrm{Epi}(f) = \{[x;c] \mid f(x) \leq c\}$. Recall that f is convex if and only if $\mathrm{Epi}(f)$ is convex. A function f is said to be lower semi-continuous (l.s.c.) if the set $\{f \leq \alpha\}$ is closed for any $\alpha \in \mathbb{R}$. Two optimization problems are *equivalent* if from a solution of one, a solution of the other is readily found, and vice versa. We denote the optimal value of an infeasible minimization problem by ∞ , see [23], [24].

B. Set representations and operations

Let C be a convex and compact polytope in \mathbb{R}^n . We consider two representations of C — H-Rep polytope (1a) and constrained zonotope (1b), respectively,

$$C = \{x \mid H_C x \le k_C\},\tag{1a}$$

$$C = \{G_C \xi + c_C \mid \|\xi\|_{\infty} \le 1, \ A_C \xi = b_C\}, \tag{1b}$$

where $H_C \in \mathbb{R}^{N_C \times n}$, $k_C \in \mathbb{R}^N_C$, $G_C \in \mathbb{R}^{n \times N_C}$, $c_C \in \mathbb{R}^n$, $A_C \in \mathbb{R}^{M_C \times N_C}$, and $b_C \in \mathbb{R}^{M_C}$. Here, (1a) is the intersection of N_C halfspaces and (1b) is an affine transformation of $\mathcal{B}_{\infty}(A_C, b_C)$, i.e., $\mathcal{C} = c_C + G_C \mathcal{B}_{\infty}(A_C, b_C)$ where

$$\mathcal{B}_{\infty}(A_C, b_C) \triangleq \{\xi \mid ||\xi||_{\infty} \le 1, A_C \xi = b_C\}.$$
 (2)

In (2), $\mathcal{B}_{\infty}(A_C, b_C)$ is the intersection of a unit-hypercube in \mathbb{R}^{N_C} with M_C linear equalities. The equivalence of the representations in (1) was recently established in [21, Thm. 1], see [21], [22] for more details.

For sets $C, S \subseteq \mathbb{R}^n$, $W \subseteq \mathbb{R}^m$, and matrix $R \in \mathbb{R}^{m \times n}$, we recall the following set operations, affine map, intersection with inverse affine map \cap_R , and Pontryagin difference \ominus :

$$RC \triangleq \{Ru \mid u \in C\},$$
 (3a)

$$\mathcal{C} \cap_R \mathcal{W} \triangleq \{ u \in \mathcal{C} \mid Ru \in \mathcal{W} \}, \tag{3b}$$

$$\mathcal{C} \ominus \mathcal{S} \triangleq \{ u \mid \forall v \in \mathcal{S}, u + v \in \mathcal{C} \}. \tag{3c}$$

Since $C \cap S = C \cap_{I_n} S$, (3b) also includes the standard intersection. We implement the *orthogonal projection* of a set $C \subset \mathbb{R}^n$ $(n_x + n_y = n)$ using (3a) and an appropriate R,

$$\operatorname{Proj}_{x}(\mathcal{C}) = \{ x \in \mathbb{R}^{n_{x}} \mid \exists y \in \mathbb{R}^{n_{y}}, \ [x; y] \in \mathcal{C} \}$$
$$= [I_{n_{x}}, 0_{n_{x} \times n_{x}}] \mathcal{C}. \tag{4}$$

We favor using constrained zonotopes (1b) over H-Rep polytopes (1a) in our work, because constrained zonotopes admit closed-form expressions for exact/inner-approximation of all set operations in (3). From [21], [22], for a zonotope $\mathcal{Z} = \{G_Z \xi + c_Z \mid \|\xi\|_{\infty} \leq 1\} \subset \mathbb{R}^n$ for $G_Z \in \mathbb{R}^{n \times N_Z}$ and $c_Z \in \mathbb{R}^n$ and a full-dimensional constrained $\mathcal{V} = (G_V, c_V, A_V, b_V)$,

$$RC = (RG_C, Rc_C, A_C, b_C), \tag{5a}$$

$$C \cap_R W = ([G_C, 0], c_C, [A_C, 0; 0, A_W; RG_C, -G_W],$$

$$[b_C; b_W; c_W - Rc_C]), (5b)$$

$$\mathcal{V} \ominus \mathcal{Z} \supseteq (G_V D, c_V - c_Z, A_V D, b_V), \tag{5c}$$

with $D \in \mathbb{R}^{N_C \times N_C}$ in (5c) as a diagonal matrix with entries $D_{ii} = 1 - \left\| e_i^\top [G_V; A_V]^\dagger [G_Z; 0_{M_V \times n}] \right\|_1$, $\forall i \in \mathbb{N}_{[1,N_V]}$ and M^\dagger as the pseudo-inverse of matrix M. Similar expressions to (5c) are also known for arbitrary p-norm balls, $p \neq 1$ [22]. In contrast, for H-Rep polytopes, only intersection (3b) and Pontryagin difference (3c) have closed-form expressions. Affine maps (3a) (including projection (4)) of a H-Rep polytope often cause numerical issues for n > 4 due to their computation complexity [4], [17].

C. Problem statements

Consider a discrete-time nonlinear dynamical system,

$$x_{t+1} = f(x_t, u_t, w_t) = Ax_t + Bu_t + Fw_t + Gg(x_t, u_t),$$
 (6)

with state $x_t \in \mathbb{R}^n$, input $u_t \in \mathbb{R}^m$, disturbance $w_t \in \mathcal{W} \subset \mathbb{R}^p$ for a convex and compact disturbance set \mathcal{W} , g is a vector of N_G convex, nonlinear, and l.s.c. functions $g_i : \mathbb{R}^n \times \mathbb{R}^m \to \mathbb{R}$ for each $i \in \mathbb{N}_{[1,N_G]}$, and appropriately dimensioned matrices A, B, F, G.

For a horizon $T \in \mathbb{N}$, consider the nonlinear ROCP,

$$\min_{u_0} \max_{w_0 \in \mathcal{W}} \dots \min_{u_{T-1}} \max_{w_{T-1} \in \mathcal{W}} \ell_f(x_T) + \sum_{t=0}^{T-1} \ell(x_t, u_t)$$
 (7a)

subject to
$$x_T \in \mathcal{X}_T$$
, (7b)

$$\forall t \in \mathbb{N}_{[0,T-1]}, \quad [x_t; u_t] \in \mathcal{Y}, \tag{7c}$$

$$\forall t \in \mathbb{N}_{[0,T-1]}, \quad x_{t+1} = f(x_t, u_t, w_t), \quad (7d)$$

for a given initial state $x_0 \in \mathbb{R}^n$. Here, $\mathcal{Y} \subset \mathbb{R}^n \times \mathbb{R}^m$ and $\mathcal{X}_T \subset \mathbb{R}^n$ are the state-input constraint and the terminal state constraint sets, and $\ell : \mathbb{R}^n \times \mathbb{R}^m \to \mathbb{R}$ and $\ell_f : \mathbb{R}^n \to \mathbb{R}$ are the stage cost and the terminal cost functions, respectively. We assume that \mathcal{Y} is convex, and that the set

$$\mathcal{U}(x) = \{ u \mid [x; u] \in \mathcal{Y} \}, \tag{8}$$

for any $x \in \mathbb{R}^n$ is compact. Here, $\mathcal{U}(x)$ is the set of admissible control at state x under the state-input constraint \mathcal{Y} . Finally, we assume that ℓ, ℓ_f are convex and l.s.c., and g, ℓ, ℓ_f are finite-valued over $\mathcal{Y}, \mathcal{Y}, \mathcal{X}_T$ respectively.

Remark 1. For the ease of notation, we do not explicitly consider time-varying costs, dynamics, and constraints in this paper. However, all the presented results can be easily extended to time-varying ℓ , ℓ , ℓ , and ℓ .

We face two challenges when solving (7): i) non-convexity arising from the nonlinear equality constraints (7d), and ii) multi-stage nature of (7). In order to obtain globally optimal solutions to (7), existing literature often uses the dynamic programming framework [1]. Specifically, it constructs a sequence of optimal value functions $V^* = \{V_t^*\}_{t=0}^T$ with $V_t^* : \mathbb{R}^n \to \mathbb{R}$ using the recursion,

$$V_t^*(x) = \min_{u \in \mathcal{U}(x)} \max_{w \in \mathcal{W}} \left(\ell(x, u) + V_{t+1}^*(f(x, u, w)) \right), \quad (9)$$

defined for $t \in \mathbb{N}_{[0,T-1]}$, and initialize (9) with $V_T^*(x) \triangleq \ell_T(x) + \mathbb{I}_{\mathcal{X}_T}(x)$. The recursion (9) is motivated by Bellman's principle of optimality, and V_t^* is referred to as the *optimal cost-to-go* [1]. Here, (9) may be viewed as T rounds of two-player games. At each round, u seeks to reduce the cost-to-go while w seeks to increase the cost-to-go, and possibly even achieve infeasibility, i.e., choose w such that $V_{t+1}(f(x,u,w)) = \infty$ for every $u \in \mathcal{U}(x)$.

Definition 1. (NONRANDOMIZED MARKOV POLICIES) [24, Ch. 8] A nonrandomized Markov (NRM) policy $\pi = \{\pi_t^*\}_{t=0}^{T-1}$ is a sequence of deterministic, state-feedback maps for the input with $\pi_t^* : \mathbb{R}^n \to \mathbb{R}^m$.

Proposition 1. The optimal controller for u that solves (7) is a NRM policy with π_t^* as the optimal solution map to the outer-minimization problem in (9).

Proposition 1, which follows from well-known selection theorems for l.s.c. functions [24], shows that (7) can be solved to global optimality using (9). However, the computation of V^* , π^* typically requires discretization (over space) of $\mathcal{Y} \subset \mathbb{R}^{n+m}$ and $\mathcal{X}_T \subset \mathbb{R}^n$, and as a result, suffers from the well-known curse of dimensionality [1].

In this paper, we consider a related nonlinear ROCP,

$$\min_{u_0} \max_{w_0 \in \mathcal{W}} \dots \min_{u_{T-1}} \max_{w_{T-1} \in \mathcal{W}} \begin{pmatrix} \ell_f(x_T) \\ + \sum_{t=0}^{T-1} \ell(x_t, u_t) \\ + \sum_{t=0}^{T-1} \alpha^\top g(x_t, u_t) \end{pmatrix}$$
(10a)
subject to (7b), (7c), (7d).

for a user-defined vector $\alpha \in \mathbb{R}^{N_G}$, $\alpha > 0$. We will discuss the role of α in Sections III-A and III-D. Similarly to (9), we

set up a sequence of optimal value functions $V^{\circ} = \{V_t^{\circ}\}_{t=0}^T$ with $V_t^{\circ} : \mathbb{R}^n \to \mathbb{R}$ using the following recursion,

$$V_t^{\circ}(x) = \min_{u \in \mathcal{U}(x)} \max_{w \in \mathcal{W}} \left(\ell(x, u) + \alpha^{\top} g(x, u) + V_{t+1}^{\circ} (f(x, u, w)) \right),$$
(11)

for $t \in \mathbb{N}_{[0,T-1]}$ with (11) initialized with $V_T^{\circ} = V_T^*$. Let π_u^+ denote the optimal NRM policy that solves (10). We obtain π_u^+ from the optimal solution map to the outer-minimization problem in (11), similarly to (7) and (9) (see Proposition 1).

In this paper, we address the following three problems:

Problem 1. Design a tractable algorithm to compute a NRM policy π_u^+ for (10) that is free from space discretization using convex optimization and computational geometry.

Problem 2. Determine sufficient conditions under which π_u^+ computed in Problem 1 is optimal for (10).

Problem 3. Determine an upper bound on the suboptimality incurred when using an optimal NRM policy π_u^+ designed for (10) to solve (7).

III. LOSSLESS CONVEXIFICATION OF NONLINEAR ROCP

In this section, we first formulate a nonlinear ROCP with augmented state and input equivalent to (10), propose a set-based, discretization-free approach to solve (10) to global optimality under certain conditions, and discuss a suboptimality bound when π_u^+ (the optimal controller for (10)) is used in (7). We conclude with a brief discussion of a tractable, almost lossless implementation of the proposed approach using constrained zonotopes.

Table I summarizes all the ROCP analyzed, the relevant notation used, and the key results presented in this paper.

A. Formulation of a nonlinear ROCP equivalent to (10)

Consider the ROCP with linear dynamics,

$$\min_{u_0^+} \max_{w_0 \in \mathcal{W}} \dots \min_{u_{T-1}^+} \max_{w_{T-1} \in \mathcal{W}} \quad (10a)$$

subject to (7b), (7c),

$$\forall t \in \mathbb{N}_{[0,T]}, \quad z_t = [x_t; c_t], \tag{12a}$$

$$\forall t \in \mathbb{N}_{[0,T-1]}, \quad u_t^+ = [u_t; \sigma_t; \gamma_t], \tag{12b}$$

$$\forall t \in \mathbb{N}_{[0,T-1]}, \quad \sigma_t = g(x_t, u_t), \tag{12c}$$

$$\forall t \in \mathbb{N}_{[0,T-1]}, \quad \gamma_t = \ell(x_t, u_t), \tag{12d}$$

$$c_T = \ell_f(x_T),\tag{12e}$$

$$\forall t \in \mathbb{N}_{[0,T-1]}, \quad z_{t+1} = A^+ z_t + B^+ u_t^+ + F^+ w_t,$$
(12f)

with an augmented state $z_t = [x_t; c_t] \in \mathbb{R}^{n+1}$, augmented input $u_t^+ = [u_t; \sigma_t; \gamma_t] \in \mathbb{R}^{m+N_G+1}$, disturbance $w_t \in \mathbb{R}^p$, same as (6), and matrices

$$A^{+} = \begin{bmatrix} A & 0_{n \times 1} \\ 0_{1 \times n} & 1 \end{bmatrix}, \tag{13a}$$

$$B^{+} = \begin{bmatrix} B & G & 0_{n \times 1} \\ 0_{1 \times m} & -\alpha^{\top} & -1 \end{bmatrix}, F^{+} = \begin{bmatrix} F \\ 0_{1 \times p} \end{bmatrix}. \quad (13b)$$

TABLE I

DIFFERENT ROCP AND SUMMARY OF RESULTS. THM. 1 PROVIDES SUFFICIENT CONDITIONS UNDER WHICH ALGO. 1 CAN SOLVE (12) (AND THEREBY, (10)) TO GLOBAL OPTIMALITY. THM. 2 BOUNDS THE SUBOPTIMALITY OF USING SUCH A CONTROLLER ON (7).

Nonlinear ROCP	(7)	(10)	(12)	
Description	Typical nonlinear ROCP	(7) with a new cost (10a)	Equivalent to (10)	
State	$x \in \mathbb{R}^n$	$x \in \mathbb{R}^n$	$z \in \mathbb{R}^{n+1}$	
Input	$u \in \mathbb{R}^m$	$u \in \mathbb{R}^m$	$u^+ \in \mathbb{R}^{m+N_G+1}$	
Opt. input policy	π^*	π_u^+	π^+	
Opt. disturbance policy	ω^*	ω^+	ω^+	
Opt. value function	$V_0^*: \mathbb{R}^n \to \mathbb{R}$	$V_0^{\circ}: \mathbb{R}^n \to \mathbb{R}$	$V_0^+: \mathbb{R}^{n+1} \to \mathbb{R}$	

By (12c) and (12f), x_t in (12) follows the nonlinear dynamics (7d). In other words, despite the introduction of an auxiliary state c_t and auxiliary inputs σ, γ , (12) has an identical feasible space for x and u as (7), and identical objectives. Thus, (10) and (12) are equivalent.

We briefly discuss the motivations of introducing $c, \alpha, \sigma, \gamma$ in (12). While constraints (12c)–(12e) are non-convex in their current form, their relaxations to $g \leq \sigma, \ell \leq \gamma, \ell_f \leq c_T$ are convex, which we will use to address Problem 1 in Section III-C. Since $\alpha > 0$, we can use the epigraph form [23, Sec. 4.1.3] to replace g with σ in (10a). From (12c), (12d), (12f), c_t satisfies the recursion,

$$c_t = \ell(x_t, u_t) + \alpha^{\top} g(x_t, u_t) + c_{t+1},$$
 (14)

for $t \in \mathbb{N}_{[0,T-1]}$ with (14) initialized by (12e). In other words, c_t is the cost-to-go function of the ROCP (10),

$$c_t = \ell_f(x_T) + \sum_{k=t}^{T-1} (\ell(x_k, u_k) + \alpha^{\mathsf{T}} g(x_k, u_k)).$$
 (15)

B. Dynamic programming recursion to analyze ROCP (12)

Similarly to (9), one can analyze and (in theory) compute the optimal policy π^+ that solves (12) using dynamic programming. Specifically, we construct a sequence of optimal value functions $V^+ = \{V_t^+\}_{t=0}^T$ with $V_t^+ : \mathbb{R}^{n+1} \to \mathbb{R}$ based on V° defined in (11) via the recursion,

$$V_{t}^{\circ}(x) = \min_{u^{+} \in \mathcal{U}_{\text{EQ}}^{+}(x)} \max_{w \in \mathcal{W}} \begin{pmatrix} \gamma + \alpha^{\top} \sigma \\ +V_{t+1}^{\circ} \left(Ax + Bu + Fw + G\sigma\right) \end{pmatrix}, \tag{16a}$$

$$V_t^+(z) = V_t^{\circ}(x) + \mathbb{I}_{\{V_t^{\circ}(x) = c\}}(z), \tag{16b}$$

for $t \in \mathbb{N}_{[0,T-1]}$ with (16a) initialized by

$$V_T^{\circ}(x) \triangleq \ell_f(x) + \mathbb{I}_{\mathcal{X}_T}(x), \tag{17}$$

 V_T^+ given by (16b), and $\mathcal{Y}_{\mathrm{EQ}}^+, \mathcal{U}_{\mathrm{EQ}}^+$ given by,

$$\mathcal{Y}_{\text{EQ}}^{+} = \left\{ [x; u^{+}] \mid \begin{array}{c} [x; u] \in \mathcal{Y}, \ \ell(x, u) = \gamma, \\ g(x, u) = \sigma \end{array} \right\}, \quad \text{(18a)}$$

$$\mathcal{U}_{\text{EQ}}^{+}(x) = \left\{ u^{+} \mid [x; u^{+}] \in \mathcal{Y}_{\text{EQ}}^{+} \right\}.$$
 (18b)

Here, (16a) is identical to (11) due to (18), while $\mathbb{I}_{\{V_t^{\circ}(x)=c\}}$ enforces $c_t=V_t^{\circ}(x_t)$ by (15) and (16b).

Algorithm 1 Set-based optimal controller synthesis for (12)

Input: Augmented linear dynamics A^+, B^+, F^+ in (12f), augmented sets \mathcal{Y}^+ and \mathcal{X}_T^+ in (21), horizon $T \in \mathbb{N}$, initial state x_0 .

Output: Input policy π^+ (19) that solves (12).

- 1: Initialize $\mathcal{K}_T \leftarrow \mathcal{X}_T^+$
- 2: **for** $t \in \{T-1,\ldots,0\}$ **do** \triangleright Robust controllable set 3: $\mathcal{K}_t \leftarrow \operatorname{Proj}_z \left(\left\{ [z;u^+] \middle| \begin{array}{c} [x;u^+] \in \mathcal{Y}^+, \\ A^+z + B^+u^+ \in \mathcal{K}_{t+1} \ominus (F^+\mathcal{W}) \end{array} \right\} \right)$
- 4: end for
- 5: **for** $t \in \{0, 1, \dots, T-1\}$ **do** \triangleright Forward roll-out
 6: Define $\pi_t^+(x_t) = [u_t^*; \sigma_t^*; \gamma_t^*]$, where $u_t^*, \sigma_t^*, \gamma_t^*$ are the optimal solutions for (20) given the current state x_t ,

minimize
$$u_{t}, \sigma_{t}, \gamma_{t}, c_{t}$$
subject to
$$u_{t} \in \mathbb{R}^{m}, \ \sigma_{t} \in \mathbb{R}^{N_{G}}, \ \gamma_{t} \in \mathbb{R}, \ c_{t} \in \mathbb{R},$$

$$A^{+} \begin{bmatrix} x_{t} \\ c_{t} \end{bmatrix} + B^{+} \begin{bmatrix} u_{t} \\ \sigma_{t} \\ \gamma_{t} \end{bmatrix} \in \mathcal{K}_{t+1} \ominus (F^{+}\mathcal{W}),$$

$$[x_{t}; u_{t}; \sigma_{t}; \gamma_{t}] \in \mathcal{Y}^{+}.$$

$$(20)$$

7: end for

The optimal input for (12) is also a NRM policy with π_t^* as the optimal solution map to the outer-minimization problem in (16a) due to compactness of $\mathcal{U}_{\mathrm{EQ}}^+(x)$ for every $x \in \mathbb{R}^n$ and l.s.c. V_t°, V_t^+ , similarly to Proposition 1. However, the outer-minimization in (16a) is non-convex, since $\mathcal{U}_{\mathrm{EQ}}^+$ requires enforcement of *convex (non-affine) equality constraints*. By (12c) and (12d), π_t^+ has the form,

$$\pi_t^+(x) = \left[\pi_{u,t}^+(x); \ g(x, \pi_{u,t}^+(x)); \ \ell(x, \pi_{u,t}^+(x)) \right], \quad (19)$$

where $\pi_u^+ = \left\{\pi_{u,t}^+\right\}_{t=0}^{T-1}$ is the optimal NRM policy for (10). As discussed in Section II-C, an implementation of (16) requires space discretization of $\mathcal{Y}_{\mathrm{EQ}}^+$ and $\mathcal{U}_{\mathrm{EQ}}^+$, and hence it is usually impractical for n>3.

C. Space discretization-free solution to ROCP (12) via sets

We consider a convex relaxation of the outer-minimization problem in (16a), where we use \mathcal{Y}^+ (a convex relaxation of $\mathcal{Y}^+_{\mathrm{EO}}$) and \mathcal{X}^+_T ,

$$\mathcal{Y}^{+} = \left\{ \left[x; u^{+} \right] \mid \left[x; u \right] \in \mathcal{Y}, \ell(x, u) \le \gamma, g(x, u) \le \sigma \right\}, \quad \text{(21a)}$$

$$\mathcal{X}_{T}^{+} = \left\{ \left[x; c \right] \mid x \in \mathcal{X}_{T}, \ \ell_{f}(x) < c \right\}. \quad \text{(21b)}$$

To avoid the scenario where u^+ computed for the convex relaxation is infeasible for (16a), we propose sufficient conditions under which the convex relaxation is *lossless*. Specifically, we propose sufficient conditions under which the nonconvex, outer-minimization problem in (16a) is equivalent to the convex formulation based on $\mathcal{Y}^+, \mathcal{X}_T^+$. Then, we use existing literature for computing robust controllable set computation to solve (16a) without any space discretization, i.e., without an explicit computation of V° .

We summarize our approach in Algorithm 1, which has two stages. First, it computes the *robust controllable set* of the linear dynamics (12f) with state-input constraints $\mathcal{Y}^+, \mathcal{X}_T^+$. For convex $\mathcal{Y}^+, \mathcal{X}_T^+$, the set recursion in Step 3 yields convex \mathcal{K}_t for each $t \in \mathbb{N}_{[0,T]}$ [4], [17]. Next, we compute the controller π_t^+ by solving (20), a convex onestep optimization problem, parameterized by x_t .

We now propose a set of sufficient conditions in Theorem 1 which guarantee that π^+ computed by Algorithm 1 is globally optimal for (12) (and thereby, (10)). We will later discuss a collection of stronger, but easier-to-check sufficient conditions based on Theorem 1.

Theorem 1. (SUFFICIENT CONDITIONS FOR LOSSLESS CONVEXIFICATION) Let the following assumptions hold. A1) for each $i \in \mathbb{N}_{[1,N_G]}$, the functions $p_a, p_b, p_c : \mathbb{R} \to \mathbb{R}$ (defined below) are non-decreasing,

A1.a) $p_a(\theta) \triangleq g_j(x + G_i\theta, u)$ is defined for all $[x; u] \in \mathcal{Y}$ for each $j \in \mathbb{N}_{[1,N_G]}$,

A1.b) $p_b(\theta) \triangleq \ell(x + G_i\theta, u)$ is defined for all $[x; u] \in \mathcal{Y}$, A1.c) $p_c(\theta) \triangleq \ell_f(x + G_i\theta)$ is defined for all $x \in \mathcal{X}_T$. A2) A and G in (12f) satisfy AG = G.

A3) for all $x \in \mathbb{R}^n$, $u, u' \in \mathbb{R}^m$, $w \in \mathbb{R}^p$, and $\sigma \geq g(x, u)$,

$$[Ax + Bu + Fw + G\sigma; u'] \in \mathcal{Y}$$

$$\Longrightarrow [Ax + Bu + Fw + Gg(x, u); u'] \in \mathcal{Y}. \tag{22}$$

A4) for all $x \in \mathbb{R}^n$, $u \in \mathbb{R}^m$, $w \in \mathbb{R}^p$, and $\sigma \geq g(x, u)$,

$$Ax + Bu + Fw + G\sigma \in \mathcal{X}_T$$

$$\Longrightarrow Ax + Bu + Fw + Gq(x, u) \in \mathcal{X}_T. \tag{23}$$

Then, the following results hold true:

R1) for each $t \in \mathbb{N}_{[0,T]}$, V_t° is convex with $\mathrm{Epi}(V_t^{\circ}) = \mathcal{K}_t$, where \mathcal{K}_t is defined in Step 3 of Algorithm 1,

R2) for each $t \in \mathbb{N}_{[0,T]}$, each $i \in \mathbb{N}_{[1,N_G]}$, and for all $[x;c] \in \mathcal{K}_t$, $p(\theta) \triangleq V_t^{\circ}(x + G_i\theta)$ is non-decreasing in θ for every θ such that $[x + G_i\theta;c] \in \mathcal{K}_t$, and

R3) starting from an initial state x_0 , for each $t \in \mathbb{N}_{[0,T-1]}$, (20) computes π_t^+ that solves (12).

In other words, Algorithm 1 addresses Problem 2.

Proof sketch. For t=T, we have R1) with the observation that $V_T=\ell_f+\mathbb{I}_{\mathcal{X}_T}$, and $\mathrm{Epi}(V_T^\circ)=\{z\mid \ell_f(x)\leq c, x\in\mathcal{X}_T\}=\mathcal{X}_T^+=\mathcal{K}_T$ by (21b) and Step 1 of Algorithm 1. R2) follows from A1.c) and A4).

For $t \in \mathbb{N}_{[0,T-1]}$, R1), R2), and R3) follows from a proof by induction.

We first focus on the base case, t = T - 1. By (13b), $c_{T-1} = c_T + \gamma_{T-1} + \alpha^{\top} \sigma_{T-1}$. By (3c) and R1) at t = T, the following constraint in (20) at t = T - 1,

$$A^{+} \begin{bmatrix} x_{T-1} \\ c_{T-1} \end{bmatrix} + B^{+} \begin{bmatrix} u_{T-1} \\ \sigma_{T-1} \\ \gamma_{T-1} \end{bmatrix} \in \mathcal{K}_{T} \ominus (F^{+}\mathcal{W}),$$

is equivalent to

$$\max_{w \in \mathcal{W}} V_T^{\circ} (Ax_{T-1} + Bu_{T-1} + Fw_{T-1} + G\sigma_{T-1}) \le c_T. \quad (24)$$

Additionally, $\alpha > 0$, the monotonicity assumptions in A1) and A3), and monotonicity result of R2) at t = T together ensure that, starting from any feasible solution of (20), we

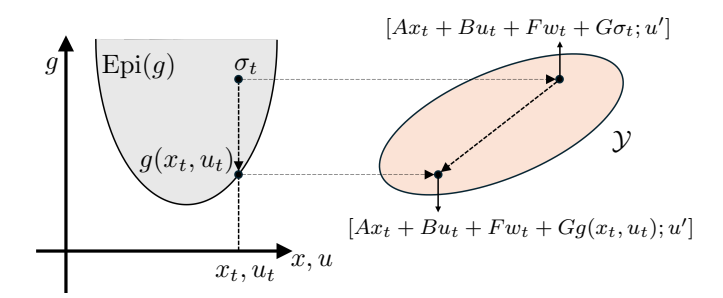


Fig. 1. Illustration of the assumption A3) in Theorem 1. Specifically, \mathcal{Y} does not prevent component-wise minimization of σ_t until $\sigma_t = g(x_t, u_t)$.

can continue decreasing γ_{T-1} and σ_{T-1} component-wise without any loss of feasibility. Consequently, minimization of c_{T-1} in (20) forces the minimization of γ_{T-1} and σ_{T-1} component-wise until they coincide with $\ell(x_{T-1},u_{T-1})$ and $g(x_{T-1},u_{T-1})$ at optimality. In other words, the optimal u^+ for (20) is also optimal for (16a), which had convex nonlinear equality constraints $g=\sigma$ and $\ell=\gamma$. Thus, the optimal value of (20) coincides with that of (16a), which completes the proof of R3) at t=T-1.

The proof of R2) for t=T-1 follows via monotonicity arguments—specifically, A1.a), A1.b), A2), A3), and R2) at t=T. Here, AG=G in A2) allows the determination of monotonicity of V_{T-1} using the monotonicity of V_T , which follows from R2) for t=T.

The proof of R1) for t = T - 1 follows from the definition of \mathcal{K}_{T-1} in Algorithm 1 and the optimal values of (20) and (16a) coincide, as proven by R3) for t = T - 1.

Using arguments similar to the base case, we can also show the induction step, i.e, R1), R2), and R3) holds for t=k when they hold for t=k+1 for some $k \in \mathbb{N}_{[0,T-1]}$. \square

We make several observations about Algorithm 1 and Theorem 1. First, from (24), observe that the outer-maximization in (16a) is encoded in Pontryagin difference $\mathcal{K}_{t+1} \ominus (F^+ \mathcal{W})$ in Algorithm 1, overcoming the bi-level optimization problem in (16a) without incurring any conservatism. Second, the non-decreasing requirement on g, ℓ, ℓ_f in A1) is similar to that of the composition rules for convex functions that preserve convexity [23]. For example, A1.a) ensures that q(f(x,u,w),u) remains convex in x,u,w. Third, as seen in Figure 1, Assumptions A3) and A4) enable reducing the auxiliary inputs σ , γ until (12c) and (12d) are active. Fourth, we have V_0^+ from \mathcal{K}_0 by (16b), i.e., for any $x_0 \in \mathbb{R}^n$, $V_0^+(x_0) = \min_{c \in \operatorname{Proj}_c(\mathcal{K}_0 \cap \{[x;c]|x=x_0\})} c$. Finally, while it is well-known that V_t° is convex with $\operatorname{Epi}(V_t^{\circ}) = \mathcal{K}_t$ for ROCP with linear dynamics [6], Theorem 1 provides sufficient conditions under which V_t° is convex with $\mathrm{Epi}(V_t^{\circ}) = \mathcal{K}_t$ for some nonlinear ROCP (12). Additionally, since projection preserves convexity, Theorem 1 also provides sufficient conditions for convexity of the robust controllable set of nonlinear dynamics (6) under constraints $\mathcal{Y}, \mathcal{X}_T$.

Corollary 1. (CONVEXITY OF ROBUST CONTROLLABLE SET) Let all assumptions in Theorem 1 hold. Then, the robust controllable set of the nonlinear dynamics (6) under

constraints $\mathcal{Y}, \mathcal{X}_T$ is the domain of V_0° , which coincides with $\operatorname{Proj}_{r}(\mathcal{K}_{0})$, the projection of the set \mathcal{K}_{0} on to \mathcal{X} .

Proposition 2. (EASY-TO-CHECK CONDITIONS FOR LOSS-LESS CONVEXIFICATION) Consider (12) with state x = $[x_{\rm L}; x_{\rm NL}] \in \mathbb{R}^{n_{\rm L}+n_{\rm NL}}$ with $n_{\rm L}+n_{\rm NL}=n$ and dynamics (6) such that

$$A = \begin{bmatrix} A_{\rm L} & 0_{n_{\rm L} \times n_{\rm NL}} \\ A_{\rm L,NL} & I_{n_{\rm NL} \times n_{\rm NL}} \end{bmatrix}, G = \begin{bmatrix} 0_{n_{\rm L} \times N_G} \\ G_{\rm NL} \end{bmatrix}, (25)$$

for some matrices $A_{L}, A_{L,NL}, G_{NL}$ that are appropriately dimensioned. Let

$$g(x, u) = g'(x_L, u), \ \ell(x, u) = \ell'(x_L, u), \ \ell_f(x) = \ell'(x_L),$$

for some convex, l.s.c, functions g', ℓ', ℓ'_f . Let \mathcal{Y} be the Cartesian product of some compact and convex set $\mathcal{Y}' \subset$ $\mathbb{R}^{n_{\rm L}+m}$ and an axis-aligned box in $\mathbb{R}^{n_{\rm NL}}$, i.e.,

$$\mathcal{Y} = \{ [x_{L}; x_{NL}; u] \mid [x_{L}; u] \in \mathcal{Y}', \Delta^{-} \le x_{NL} \le \Delta^{+}_{Y, NL} \},$$

with $\Delta^-, \Delta^+_{Y,NL} \in \mathbb{R}^{n_{NL}}$ for some $\Delta^+_{Y,NL} \geq \Delta^-$,

$$\Delta_i^- = \min_{[x_{\mathrm{L}}: u] \in \mathcal{Y}'} e_i^\top G_{\mathrm{NL}} g(x_{\mathrm{L}}, u), \qquad \forall i \in \mathbb{N}_{[1, n_{\mathrm{NL}}]}, \quad (26)$$

and e_i are the standard axis vectors of $\mathbb{R}^{n_{\rm NL}}$. Let \mathcal{X}_T be the Cartesian product of some compact and convex set $\mathcal{X}'_T \subset$ $\mathbb{R}^{n_{\rm L}}$ and an axis-aligned box in $\mathbb{R}^{n_{\rm NL}}$,

$$\mathcal{X}_T = \{ [x_L; x_{NL}] \mid x_L \in \mathcal{X}_T', \Delta^- \le x_{NL} \le \Delta_{X,NL}^+ \},$$

for some $\Delta^+_{X,NL} \in \mathbb{R}^{n_{NL}}, \Delta^+_{X,NL} \geq \Delta^-$. Then, all the results in Theorem 1 and Corollary 1 hold.

Proposition 2 characterizes a broad class of nonlinear ROCP using easy-to-check sufficient conditions for which Algorithm 1 solves (10) to global optimality. Specifically, it partitions the state space based on the dynamics (6) into two components — $x_{
m L}$ that follows linear dynamics and $x_{\rm NL}$ that follows nonlinear dynamics. Here, (25) satisfies A2). Additionally, Proposition 2 requires the nonlinear terms in (6) to be only a function of x_L and u, which satisfies A1) without imposing any monotonicity requirements on g', ℓ', ℓ'_f . Finally, since Δ^- in (26) is the (component-wise) minima of $G_{\rm NL}g$ over \mathcal{Y}' , the definition of \mathcal{Y} and \mathcal{X}_T in Proposition 2 satisfies A3) and A4). In Section IV, we consider a numerical example that satisfies Proposition 2.

D. Suboptimality bounds for π_n^+ when used to solve (7)

We now turn our attention to Problem 3. Similarly to the definition of π^+ in (19), we define a NRM policy π^{\dagger} that is feasible but possibly suboptimal for (12) using π^* ,

$$\pi_t^{\dagger}(x) = [\pi_t^*(x); \ g(x, \pi_t^*(x)); \ \ell(x, \pi_t^*(x))],$$
 (27)

with π_t^{\dagger} defined for all $x \in \mathbb{R}^n, t \in \mathbb{N}_{[0,T-1]}$, and $\pi_u^{\dagger} = \pi^*$. We define a real-valued function L and a N_G -valued function C,

$$L(\pi,\omega;x_0) \triangleq \ell_f(x_T) + \sum_{t=0}^{T-1} \ell(x_t, \pi_t(x_t)), \qquad (28)$$

$$L(\pi, \omega; x_0) \triangleq \ell_f(x_T) + \sum_{t=0}^{T-1} \ell(x_t, \pi_t(x_t)), \qquad (28)$$

$$C(\pi, \omega; x_0) \triangleq \sum_{t=0}^{T-1} g(x_t, \pi_t(x_t)). \qquad (29)$$

where $\{x_t\}_{t=0}^T$ is the trajectory of (6) under π and ω .

Let the optimal disturbance policy for (7) and (12) be ω^* and ω^+ . Then, for a given initial state x_0 , we have

$$V_0^*(x_0) = L(\pi^*, \omega^*; x_0), \tag{30}$$

$$V_0^+(x_0) = L(\pi^+, \omega^+; x_0) + \alpha^\top C(\pi^+, \omega^+; x_0).$$
 (31)

For brevity, we drop references to x_0 in L, C hereafter.

Theorem 2. (SUBOPTIMALITY GAP) The suboptimality incurred when using π_u^+ to solve (7) is bounded,

$$0 \le L(\pi_u^+, \omega^*) - L(\pi^*, \omega^*) \le \alpha^\top (C(\pi^*, \omega^+) - C(\pi^+, \omega^+)).$$

Proof. We observe that

$$L(\pi^*, \omega^*) \le L(\pi_u^+, \omega^*), \tag{32a}$$

$$L(\pi^*, \omega^+) \le L(\pi^*, \omega^*), \tag{32b}$$

$$L(\pi_u^+, \omega^+) + \alpha^\top C(\pi_u^+, \omega^+) \le L(\pi^*, \omega^+) + \alpha^\top C(\pi^*, \omega^+), \quad (32c)$$

$$L(\pi_u^+, \omega^*) + \alpha^\top C(\pi_u^+, \omega^*) \le L(\pi_u^+, \omega^+) + \alpha^\top C(\pi_u^+, \omega^+).$$
 (32d)

Here, (32a) and (32b) follows from the optimality of π^* and ω^* over π_u^+ and ω^+ for (7), and (32c) and (32b) follows from the optimality of π^+ and ω^+ over π^* and ω^* for (12). We have the lower bound from (32a), and obtain the upper bound starting from (32d) and applying (32c) and (32b). \Box

Theorem 2 addresses Problem 3, and shows that solving (12) to global optimality is sufficient to solve (7) with bounded suboptimality. The suboptimality decreases as the gap between the nonlinear terms g in (6) shrinks for the NRM policies π^* and π^+ under the optimal disturbance policy ω^+ for (12). Additionally, the suboptimality decreases as $\|\alpha\| \to 0$, which is expected from the relationship between (7) and (10) (thereby, (12)). But we note that one may face numerical issues when implementing Algorithm 1 for extremely small α .

E. An almost lossless implementation of Algorithm 1

We briefly discuss why an exact implementation of Algorithm 1 that is lossless is challenging and how a constrained zonotope-based implementation yields an almost lossless implementation. While $\mathcal{Y}^+, \mathcal{X}_T^+$ in (21) themselves are not compact, we can add loose upper-bounds on c, σ, γ to render these sets compact without incurring any approximation.

For convex, piecewise-affine functions g_i , i $\mathbb{N}_{[1,N_G]}, \ell, \ell_f$, and polytopes $\mathcal{Y}, \mathcal{X}_T$ in (12), the sets \mathcal{Y}^+ and \mathcal{X}_T^+ in (21) are polytopes. Consequently, Step 3 may be implemented exactly using operations on polytopes in existing toolboxes [18]-[20], and we can solve (12) to global optimality by Algorithm 1 under the sufficient conditions in Theorem 1. Such an implementation is exact, and therefore lossless. However, a tractable implementation of Algorithm 1 using the standard H-Rep representations (1a) is hindered by the need to compute projections, which is a computationally expensive operation for H-Rep polytopes. On the other hand, constrained zonotopes (1b) are equivalent to H-Rep polytopes, and admit closed-form expressions for all the set operations necessary for Step 3 and (20) (see Section II-B). Since (5c) yields an inner-approximation (that is exact in some cases [22]), we have an *almost lossless* implementation of Algorithm 1 with constrained zonotopes.

When $g_i, i \in \mathbb{N}_{[1,N_G]}, \ell, \ell_f$ are convex but not piecewise-affine, the sets \mathcal{Y}^+ and \mathcal{X}_T^+ are no longer polytopes. However, their epigraphs are convex, and may be outer/inner-approximated by polytopes (or constrained zonotopes) to arbitrary accuracy via ray-shooting [25]. As a concrete example, consider $\ell_f : \mathbb{R}^n \to \mathbb{R}$ with $\ell_f(x) = \|x\|_2$. Here, $\mathrm{Epi}(\ell_f) = \{[x;c] \mid \ell_f(x) \leq c\} = \{[x;c] \mid \|x\|_2 \leq c\}$ is a second-order cone [23]. For $\{v_i\}_{i=1}^{N_V}$ that are $N_V \in \mathbb{N}$ distinct points on the boundary of the unit sphere in \mathbb{R}^n ,

$$\operatorname{Epi}(\ell_f) \supset \left\{ [x; c] \mid x \in \operatorname{ConvexHull}\left(\left\{ cv_i \right\}_{i=1}^{N_V} \right) \right\}, \quad \ (33a)$$

$$\operatorname{Epi}(\ell_f) \subset \{ [x; c] \mid \forall i \in \mathbb{N}_{[1, N_V]}, \ v_i^\top x \le c \}, \tag{33b}$$

where the approximations becomes tighter (in volume) as N_V increases. See [25] for an optimization-based computation of v_i . To ensure convexity in [x; c], we cast (33a) as,

$$\left\{ [x;c] \mid x \in \text{ConvexHull}\left(\left\{cv_i\right\}_{i=1}^{N_V}\right) \right\}$$

$$= \left\{ [x;c] \mid \phi \ge 0, \ \mathbf{1}_{N_V}^{\top} \phi = c, \ \sum_{i=1}^{N_V} \phi_i v_i = x \right\}. \tag{34}$$

When inner-approximations of $\mathcal{Y}^+, \mathcal{X}_T^+$ are used, Algorithm 1 yields a feasible but suboptimal solution to (12) with conservatism arising from (34) and (5c). While the user controls the conservatism from (34) via N_V , the effect of (5c) on Algorithm 1 requires further investigation. When outer-approximations of $\mathcal{Y}^+, \mathcal{X}_T^+$ are used along with [22, Alg. 5] (outer-approximation of $\mathcal{V} \ominus \mathcal{Z}$), we obtain a super-optimal solution to (12) that can help quantify the sub-optimality of the inner-approximation approach.

IV. NUMERICAL EXAMPLE

We consider a monitoring application using an energy-constrained drone. The mission specification requires the drone to approach a static target located at $p_{\text{target}} \in \mathbb{R}^3$ for monitoring, and subsequently return to a pre-specified terminal location $p_{\text{terminal}} \in \mathbb{R}^3$, while subject to wind disturbances. We model the limited onboard battery by a hard constraint on the cumulative sum of thrust magnitudes.

We model the drone dynamics as a 3D double integrator with position $p_t \in \mathbb{R}^3$ and velocity $v_t \in \mathbb{R}^3$ and acceleration $u_t \in \mathbb{R}^3$ at time $t \in \mathbb{N}$, discretized in time via a zero-order hold with sampling time Δ_t . We model the acceleration due to wind disturbances by $w_t \in \mathbb{R}^3$. Additionally, we denote the cumulative sum of thrust magnitudes $b_t = b_0 + \sum_{k=0}^{t-1} \|u_k\|_2$, for $t \in \mathbb{N}_{[1,T]}$, which may be equivalently expressed by $b_{t+1} = b_t + \|u_t\|_2$. Thus, the dynamics of the system in the form (6) are,

$$x_{t+1} = f(x_t, u_t, w_t) = Ax_t + Bu_t + Fw_t + G||u_t||_2, \quad (35)$$

with state $x_t = [p_t; v_t; b_t]$, input $u_t \in \mathbb{R}^3$, disturbance $w_t \in \mathcal{W} \subset \mathbb{R}^3$, $N_G = 1$, $g(x, u) = ||u||_2$, F = B, and

$$A = \begin{bmatrix} I_3 & \Delta_t I_3 & 0_{3\times 1} \\ 0_{3\times 3} & I_3 & 0_{3\times 1} \\ 0_{1\times 3} & 0_{1\times 3} & 1 \end{bmatrix}, B = \begin{bmatrix} \frac{\Delta_t^2}{2} I_3 \\ \Delta_t I_3 \\ 0_{1\times 3} \end{bmatrix}, G = \begin{bmatrix} 0_{6\times 1} \\ 1 \end{bmatrix}.$$

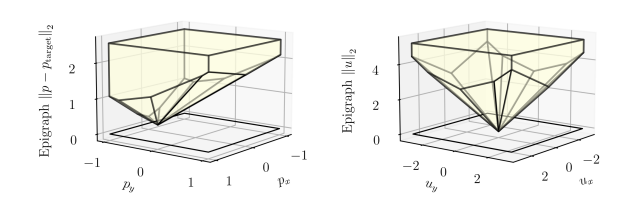


Fig. 2. Epigraph of ℓ and g for $p_z = 0.5$ and $u_z = 0$ using (34). The set in the xy plane shows the constraints on $[p_x; p_y]$, $[u_x; u_y]$ from \mathcal{Y} .

We model the nonlinear ROCP using (12) with,

$$\ell_f(x) = \ell(x, u) = \ell(p) = \|p - p_{\text{target}}\|_2,$$
 (36a)

$$\mathcal{Y} = \left\{ [x; u] \middle| \begin{array}{l} [-1; -1; 0] \le p \le [1; 1; 2], \\ \|v\|_{\infty} \le 1, \ 0 \le b \le \Delta_B, \ \|u\|_{\infty} \le 3 \end{array} \right\}, \quad (36b)$$

$$\mathcal{X}_T = \{ x \mid ||[p - p_{\text{terminal}}; v]||_{\infty} \le 0.1, \ 0 \le b \le \Delta_B \}.$$
 (36c)

Here, (10a) is a weighted sum of the tracking error and the cumulative sum of thrust magnitudes at the end of the mission. (35) and (36) together satisfy Proposition 2, which guarantees that Algorithm 1 solves (12) to global optimality.

We set up and solve (12) with T=30, $\Delta_t=0.1$, $p_0=[-1;0;0]$ with zero initial velocity, $p_{\text{terminal}}=[1;0;0]$, $p_{\text{target}}=[0;-0.8;0.5]$, and $\mathcal{W}=\{w\mid \|w\|_{\infty}\leq 0.25\}$. Here, $U_{\text{max}}=\max_{u\in\operatorname{Proj}_u\mathcal{Y}}\|u\|_2=5.2$ is the maximum thrust magnitude that may be applied at any time step, $\Delta_B=0.4(U_{\text{max}}T)=62.35$ limits the cumulative sum of thrust magnitudes employed over the mission to 40% of the maximum allowed limit, and $\ell_{\text{max}}=\max_{[x;u]\in\mathcal{Y}}\ell(x,u)=2.55$ is the maximum tracking error. We set $\alpha=0.001\times 1_{N_G\times 1}$.

Figure 2 shows the epigraph of ℓ and g for fixed p_z and u_z respectively constructed using (34) for $N_V=60$. Recall that N_V in (34) is the number of vertices used to approximate the epigraph. We implemented Algorithm 1 on a standard desktop (Intel CPU i9-12900KF, 64 GB RAM) in Python 3.10 using pycvxset [20], GUROBI [26], and cvxpy [27].

We evaluate six scenarios obtained by considering three initial cumulative sum of thrust magnitudes $b_0 \in \{0, 2.5, 5\}$, with two wind conditions: (i) adversarial disturbance and (ii) no wind. Thus, the scenarios are 1.i and 1.ii with $b_0 = 0$, 2.i and 2.ii with $b_0 = 2.5$, and 3.i and 3.ii with $b_0 = 5$.

Since each scenario corresponds to different x_0 , we reuse the set recursion in Algorithm 1 (Step 3) across scenarios for a fixed N_V , and evaluate π^+ for each scenario via separate forward roll-outs (Step 6). We compute the adversarial w_t by computing the vertex of \mathcal{W} that maximizes V_{t+1}° at each iteration of (20). This approximates the optimal adversarial disturbance ω^+ via a one-step optimal disturbance policy. Exact computation of ω^+ requires space discretization [1].

Table II reports various metrics for each scenario and $N_V \in \{60, 360\}$. As expected, the approximation error significantly reduces for larger N_V at the expense of increased computations. Moreover, Scenario 3 does not have a solution for $N_V = 60$. On the other hand, the cumulative tracking error and cumulative thrust exhibit minimal variation with N_V , suggesting that the convex-hull approximation in (34) with lower N_V may be sufficient to solve (12) in some cases.

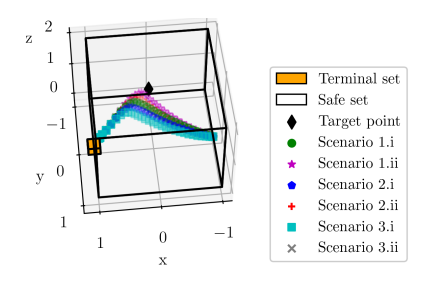


Fig. 3. Trajectories for various scenarios for $N_V = 360$.

TABLE II

Evaluation of Algorithm 1 for each scenario, $N_V \in \{60, 360\}$ on the cumulative tracking error and thrust magnitudes, relative approximation error percentage

((0.1/0.5/0.9)-quantiles) of σ, γ , and overall compute time for the two parts of Algorithm 1.

N_V	Scenario	Cumulative metric		Relative approximation error %		Compute time (s)	
		Tracking	Thrust	$(\sigma - u _2)/U_{max}$	$(\gamma - \ell(x))/\ell_{\text{max}}$	\mathcal{K}_t	π^+
60	1.i	25.26	48.23	0.0 / 0.3 / 2.0	0.2 / 0.7 / 1.4	4.79	6.35
	1.ii	23.09	47.34	0.0 / 0.1 / 1.8	0.2 / 0.7 / 1.4		8.69
	2.i	26.79	50.81	0.0 / 0.3 / 2.2	0.4 / 0.8 / 1.4		5.67
	2.ii	24.48	48.13	0.0 / 0.3 / 2.2	0.2 / 0.7 / 1.4		8.70
	3.i			INFEASIBLE			N/A
	3.ii			INFEASIBLE			N/A
360	1.i	24.42	49.33	0.0 / 0.1 / 0.5	0.1 / 0.2 / 0.4	41.20	36.58
	1.ii	22.30	50.39	0.0 / 0.0 / 0.4	0.0 / 0.2 / 0.4		38.52
	2.i	25.76	50.45	0.0 / 0.1 / 0.5	0.1 / 0.2 / 0.4		37.83
	2.ii	23.57	50.32	0.0 / 0.0 / 0.5	0.1 / 0.2 / 0.4		35.88
	3.i	27.37	52.20	0.0 / 0.1 / 0.5	0.1 / 0.2 / 0.4		38.18
	3.ii	24.95	50.48	0.0 / 0.0 / 0.5	0.1 / 0.2 / 0.4		44.15

Algorithm 1 solves the feasible four scenarios of (12) in under 14 seconds for $N_V=60$, and every scenario in under 86 seconds for $N_V=360$. As expected, the tracking error is lowest in Scenario 1.ii (no disturbance case) with $b_0=0$, and worst in Scenario 3.i — (adversarial disturbance case) with $b_0=5$ which reduces the (effective) budget for b_T .

Figure 3 shows the trajectory of the drone for each scenario. All trajectories reach the terminal set \mathcal{X}_T (orange) while satisfying \mathcal{Y} . As expected, scenarios with disturbance and lower budget show higher deviation from the target point.

Figure 4 shows that the lossless convexification guarantee from Proposition 2 holds, as expected. Specifically, despite solving a convex relaxation of (12), Algorithm 1 computes an optimal policy that has the form of (19) which satisfies (12c) and (12d) at all time steps.

V. CONCLUSION

We introduced a set-based control design framework to compute globally optimal controllers for a class of nonlinear

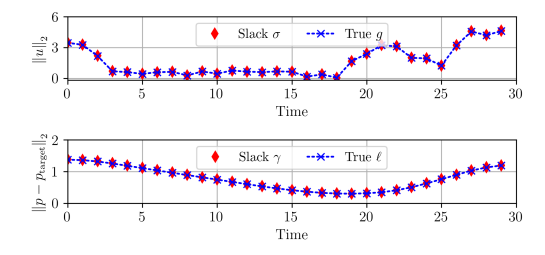


Fig. 4. Plot showing that $\sigma, g(x,u)$ (top) and $\gamma, \ell(x,u)$ (bottom) coincide for $N_V=360$ and Scenario 1.i for every $t\in\mathbb{N}_{[0,T]}$. This is due to the lossless convexification guarantee in Theorem 1.

ROCP. We demonstrated that the discretization-free approach has low computational burden using constrained zonotopes. Our future work will investigate completely lossless tractable implementation of Algorithm 1.

REFERENCES

- [1] D. Bertsekas, Dynamic programming and optimal control: Volume I. Athena scientific, 2012, vol. 4.
- [2] A. Bemporad and M. Morari, "Robust model predictive control: A survey," in *Robustness Ident. Ctrl.* Springer, 2007, pp. 207–226.
- [3] D. Mayne, "Constrained model predictive control: Stability and optimality," *Automatica*, vol. 36, no. 6, pp. 789–814, 2000.
- [4] F. Borrelli, A. Bemporad, and M. Morari, Predictive control for linear and hybrid systems. Cambridge University Press, 2017.
- [5] W. Powell, Approximate Dynamic Programming: Solving the curses of dimensionality. John Wiley & Sons, 2007, vol. 703.
- [6] E. Kerrigan and D. Mayne, "Optimal control of constrained, piecewise affine systems with bounded disturbances," in *Proc. Conf. Dec. & Ctrl.*, vol. 2, 2002, pp. 1552–1557.
- [7] D. Mayne, E. Kerrigan, E. Van Wyk, and P. Falugi, "Tube-based robust nonlinear model predictive control," *J. Robust & Nonlin. Ctrl.*, vol. 21, no. 11, pp. 1341–1353, 2011.
- [8] J. Köhler, M. Müller, and F. Allgöwer, "A novel constraint tightening approach for nonlinear robust model predictive control," in *Proc. Amer. Ctrl. Conf.*, 2018, pp. 728–734.
- [9] P. Campo and M. Morari, "Robust model predictive control," in *Proc. Amer. Ctrl. Conf.*, 1987, pp. 1021–1026.
- [10] L. Magni, G. De Nicolao, R. Scattolini, and F. Allgöwer, "Robust model predictive control for nonlinear discrete-time systems," *J. Ro*bust & Nonlin. Ctrl., vol. 13, no. 3-4, pp. 229–246, 2003.
- [11] D. Raimondo, D. Limon, M. Lazar, L. Magni, and E. Camacho, "Min-max model predictive control of nonlinear systems: A unifying overview on stability," *Euro. J. Ctrl.*, pp. 5–21, 2009.
- [12] P. Scokaert and D. Mayne, "Min-max feedback model predictive control for constrained linear systems," *IEEE Trans. Autom. Ctrl.*, vol. 43, no. 8, pp. 1136–1142, 1998.
- [13] A. Bemporad, F. Borrelli, and M. Morari, "Min-max control of constrained uncertain discrete-time linear systems," *IEEE Trans. Autom. Ctrl.*, vol. 48, no. 9, pp. 1600–1606, 2003.
- [14] D. Malyuta, T. Reynolds, M. Szmuk, T. Lew, R. Bonalli, M. Pavone, and B. Açıkmeşe, "Convex optimization for trajectory generation: A tutorial on generating dynamically feasible trajectories reliably and efficiently," *IEEE Ctrl. Syst. Mag.*, vol. 42, pp. 40–113, 2022.
- [15] B. Acikmese and S. Ploen, "Convex programming approach to powered descent guidance for mars landing," J. Guid. Ctrl. & Dyn., vol. 30, no. 5, pp. 1353–1366, 2007.
- [16] L. Blackmore, B. Açıkmeşe, and J. Carson III, "Lossless convexification of control constraints for a class of nonlinear optimal control problems," Syst. & Ctrl. Lett., vol. 61, no. 8, pp. 863–870, 2012.
- [17] F. Blanchini and S. Miani, Set-theoretic methods in control. Springer, 2008.
- [18] M. Herceg, M. Kvasnica, C. Jones, and M. Morari, "Multi-parametric toolbox 3.0," in *Proc. Euro. Ctrl. Conf.*, 2013, pp. 502–510.
- [19] M. Althoff, "An introduction to cora 2015," in Proc. Sec. Verif. Cont. Hybrid Syst., 2015, pp. 120–151.
- [20] A. Vinod, "pycvxset: A Python package for convex set manipulation," in *Proc. Amer. Ctrl. Conf.*, 2025, pp. 2515–2521.
- [21] J. Scott, D. Raimondo, G. Marseglia, and R. Braatz, "Constrained zonotopes: A new tool for set-based estimation and fault detection," *Automatica*, vol. 69, pp. 126–136, 2016.
- [22] A. Vinod, A. Weiss, and S. Di Cairano, "Projection-free computation of robust controllable sets with constrained zonotopes," *Automatica*, vol. 175, p. 112211, 2025.
- [23] S. Boyd and L. Vandenberghe, Convex optimization. Cambridge Univ. Press, 2004.
- [24] D. Bertsekas and S. Shreve, *Stochastic optimal control: the discrete-time case*. Athena Scientific, 1996, vol. 5.
- [25] J. Gleason, A. Vinod, and M. Oishi, "Lagrangian approximations for stochastic reachability of a target tube," *Automatica*, vol. 128, 2021.
- [26] Gurobi Opt., LLC, "Gurobi Optimizer Reference Manual," https://www.gurobi.com (Last accessed: 2023).
- [27] S. Diamond and S. Boyd, "CVXPY: A Python-embedded modeling language for convex optimization," *J. Mach. Learn. Res.*, vol. 17, no. 83, pp. 1–5, 2016.